RAA 2018 Vol. **18** No. **3**, 25(8pp) doi: 10.1088/1674–4527/18/3/25

http://www.raa-journal.org *http://iopscience.iop.org/raa*

***R**esearch in*
***A**stronomy and*
***A**strophysics*

Neutron stars: a relativistic study

Mehedi Kalam[1], Sk. Monowar Hossein[2] and Sajahan Molla[1]

[1] Department of Physics, Aliah University, II-A/27, New Town, Kolkata - 700156, India; *kalam@associates.iucaa.in*
[2] Department of Mathematics, Aliah University, II-A/27, New Town, Kolkata - 700156, India

Received 2017 July 10; accepted 2017 November 20

Abstract We study the inner structure of a neutron star from a theoretical point of view and the outcome results are compared with observed data. We propose a stiff equation of state relating pressure with matter density. From our study we calculate mass (M), compactness (u) and surface redshift (Z_s) for two binary millisecond pulsars, namely PSR J1614–2230 and PSR J1903+327, and four X-ray binaries, namely Cen X-3, SMC X-1, Vela X-1 and Her X-1, and compare them with recent observational data. Finally, we examine the stability for such a type of theoretical structure.

Key words: stars: neutron — stars: mass function — equation of state

1 INTRODUCTION

Studies of compact objects like neutron stars have attracted much attention among astrophysicists over the last few decades. This topic plays a crucial role that acts as a bridge among astrophysics, nuclear physics and particle physics. One type of compact object in our universe is a neutron star (or strange star). Neutron stars are the most common and well-understood compact objects for the study of dense matter physics. In general, neutron stars are composed almost entirely of neutrons, while strange stars may be made from strange quark matter (SQM) (Drago et al. 2014; Haensel et al. 1986). If we consider SQM to be stable then strange stars may be formed during supernova explosions. As a consequence of this, neutron stars could be converted to strange stars by a number of different mechanisms such as: (a) pressure-induced transformation to uds-quark matter via ud-quark matter; (b) sparking by high-energy neutrinos; (c) triggering due to the intrusion of a quark nugget. All of these possibilities were described by Alcock et al. (1986). Some scientists believe that much more rapid cooling of SQM in strange stars (in the absence of a pion condensate) takes place than in neutron stars due to neutrino emitting weak interactions involving quarks (Alcock et al. 1986). Therefore, a strange star is thought to be much colder than a neutron star of similar age. But in some cases, strange-matter stars may cool slowly and their surface temperatures are more or less indistinguishable from those of slowly cooling neutron stars (Schaab et al. 1997; Weber 2005; Page et al. 2006). The famous scientist Witten (1984) concluded that "If quark matter is stable, it is probably necessary to assume that ordinary neutron stars are really quark stars."

The state of super-dense matter above the nuclear matter density is essential for us to explore the nature of compact stars. Conventional quark matter is characterized by the soft equation of state (EOS), and the emergence of quark matter inside compact stars is usually thought to be a reason for lowering their maximum mass. But the case of quark-cluster matter could have a stiff EOS due to strong coupling (Guo et al. 2014; Lai & Xu 2009). Lai & Xu (2009) found that the Lennard-Jones model has a stiffer EOS, which leads to higher maximum masses for quark stars. In their model, they consider quarks to be grouped in clusters and these clusters are non-relativistic particles. If the intercluster potential can be described in the Lennard-Jones form, the EOS can be very stiff, because at a small intercluster distance (i.e. the number density is large enough), there is very strong repulsion.

Recently, neutron stars have been detected in binary systems in the Milky Way but only very few of

this kind of system have been identified in globular clusters. Some examples of known compact star systems (with neutron stars) are PSR J1614–2230, PSR J1903+327, Cen X-3, SMC X-1 (this is in the "Small Magellanic Cloud"), Vela X-1 and Her X-1 (Demorest et al. 2010; Freire et al. 2011; Rawls et al. 2011; Coe et al. 2013). Several researchers have studied (Rahaman et al. 2012a,b, 2014; Kalam et al. 2012, 2013a,b, 2014b,c,a; Hossein et al. 2012, 2016; Lobo 2006; Bronnikov & Fabris 2006; Egeland 2007; Dymnikova 2002; Maurya et al. 2016; Dayanandan et al. 2016; Maharaj et al. 2014; Ngubelanga et al. 2015; Pant et al. 2014; Bhar & Rahaman 2015) compact stars in different directions. In addition, scientists have used different techniques such as computational, observational or theoretical analysis to study these astrophysical objects. Because of uncertainty about the behavior of matter inside compact stars ("normal matter for neutron stars" or "SQM for strange stars"), their physical structure and some physical properties can be obtained by applicable analytic solutions of Einstein's gravitational field equations. It can also be mentioned here that because of this difficulty, a pulsar's inner structure could be modeled by the neutron star model, strange star model or even others (e.g., strangeon star model (Lai & Xu 2017)). The relativistic stellar model was studied by Schwarzschild et al. (1916), the first solution of Einstein's field equation for the interior of a compact object which is in hydrostatic equilibrium. In this regard, an important investigation was done by Tolman (1939). In his paper, he proposed eight evident analytical solutions of the field equations. Clifford E. Rhoades, Jr. and Rhoades & Ruffini (1974) showed that the maximum possible mass of a neutron star cannot be larger than 3.2 $M_{\odot}$. Buchdahl (1959) also contributed an important study on fluid spheres by obtaining the famous bound on the mass (M) − radius (R) ratio for stable general relativistic spheres, which is $\frac{2GM}{c^2R} \leq \frac{8}{9}$. In spite of the considerable progress in recent years, still there are some important features that need to be addressed about neutron stars. It can be noted that a few dozen neutron star masses have been determined accurately (to some extent) in binaries containing pulsars (Lattimer & Prakash 2005; Heap & Corcoran 1992; Stickland et al. 1997; Orosz & Kuulkers 1999; van Kerkwijk et al. 1995), but little information about their radii is available for these stars. This is because determination of radii for compact objects is very difficult.

Motivated by the above facts, we are introducing a theoretical model of neutron stars from which we can determine the mass, compactness and surface redshift of various neutron stars. Also, we are able to present a possible EOS for the stellar structure relating pressure and matter density of the star. The solution presented in this article satisfies all the energy conditions, stellar equation (some authors call this the Tolman-Oppenheimer-Volkoff (TOV) equation) and the Buchdahl mass−radius relation (Buchdahl 1959). It also satisfies other stability conditions like speed of sound, $v^2 = \frac{dp}{d\rho} < 1$, inside the star and adiabatic index, $\gamma > \frac{4}{3}$, for radial adiabatic perturbations. Interestingly, the star mass, compactness and surface redshift calculated from our model match the observed data well, which confirms the validity of our model.

We organize the article as follows: In Section 2, we discuss the interior spacetime and behavior of the star. In Section 3, we study some special features of the star, namely the stellar equation, energy conditions, stability, matching conditions, mass−radius relation, compactness and surface redshift in different subsections. In Section 4, the article concludes with a short discussion using numerical data. Before we start, it is worth mentioning that we use geometric units $G = c = 1$ throughout the article.

2 INTERIOR SPACETIME OF A STAR

In our stellar model, we consider a static and spherically symmetric matter distribution whose interior spacetime can be described by

$$ds^2 = -e^{\nu(r)}dt^2 + e^{\lambda(r)}dr^2 + r^2(d\theta^2 + sin^2\theta d\phi^2)\,. \quad (1)$$

According to Heintzmann (1969),

$$e^{\nu} \;=\; A^2\left(1+ar^2\right)^3 \quad (2)$$

and

$$e^{-\lambda} \;=\; \left[1-\frac{3ar^2}{2}\left(\frac{1+C\left(1+4ar^2\right)^{-\frac{1}{2}}}{1+ar^2}\right)\right], \quad (3)$$

where A (dimensionless), C (dimensionless) and a (length^{-2}) are constants (using $G = c = 1$).

The matter within the star will be considered a perfect fluid (locally) and consequently the energy momentum tensor for the fluid distribution can be written as

$$T^i_j = (\rho + p)v^i v_j - p\delta^i_j, \quad (4)$$

where v^i is the four velocity, ρ is the matter density and p is the fluid pressure.

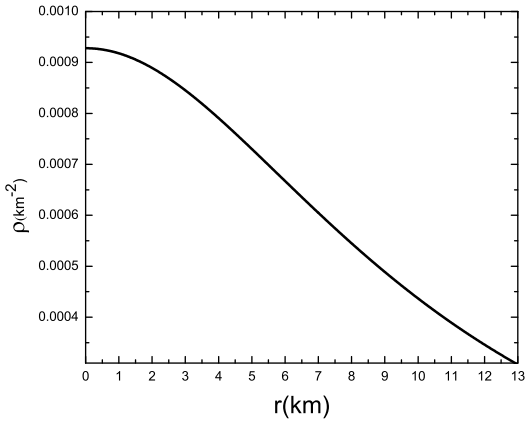

Fig. 1 Matter density (ρ) $-$ radius (r) relation in the stellar interior (taking a=0.0037 km^{-2}, C=0.4).

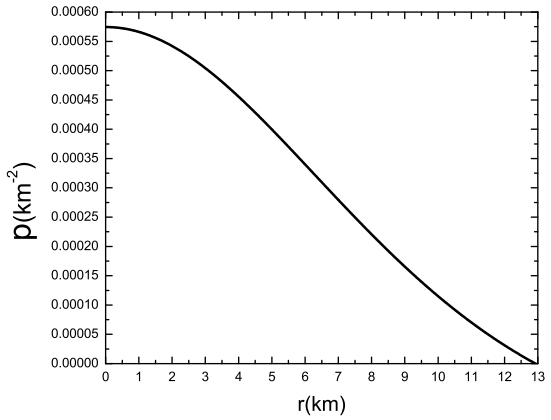

Fig. 2 Pressure (p) $-$ radius (r) relation in the stellar interior (taking $a = 0.0037\,\mathrm{km}^{-2}$, $C = 0.4$).

Solving the Einstein's field equation we get

$$\rho = \frac{3a\left(\sqrt{1+4ar^2}\left(3+13ar^2+4a^2r^4\right)+C\left(3+9ar^2\right)\right)}{16\pi\left(1+ar^2\right)^2\left(1+4ar^2\right)^{\frac{3}{2}}},$$

$$\rho_0 = \rho(r=0) = \frac{3a\left(3+3C\right)}{16\pi},$$

and

$$p = \frac{-3a\left(3\sqrt{1+4ar^2}\left(-1+ar^2\right)+C+7aCr^2\right)}{16\pi\left(1+ar^2\right)^2\left(1+4ar^2\right)^{\frac{1}{2}}},$$

$$p_0 = p(r=0) = \frac{3a\left(3-C\right)}{16\pi},$$

where ρ_0 and p_0 are the central density and central pressure of the star respectively.

We observe that pressure and matter density are maximum at the center and decrease monotonically towards the boundary (Figs. 1 and 2). Therefore, they are well behaved in the interior of the stellar structure. It can be noted that we set the values of the constants, $a = 0.0037\,\mathrm{km}^{-2}$ and $C = 0.4$, such that the pressure drops from its maximum value (at the center) to zero at the boundary.

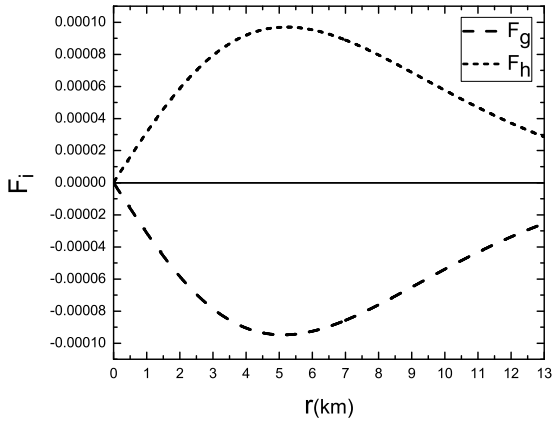

Fig. 3 Gravitational and hydrostatic forces in the stellar interior.

3 SOME SPECIAL FEATURES

3.1 Stellar Equation

The stellar equation (a modified form of the TOV equation) describes the equilibrium condition for a compact star subject to gravitational (F_{g}) and hydrostatic (F_{h}) forces,

$$F_{\mathrm{h}} + F_{\mathrm{g}} = 0, \tag{5}$$

where,

$$F_{\mathrm{g}} = -\frac{1}{2}\nu'\left(\rho+p\right), \tag{6}$$

$$F_{\mathrm{h}} = -\frac{dp}{dr}. \tag{7}$$

Therefore, static equilibrium configurations do exist in the presence of gravitational and hydrostatic forces (Fig. 3).

3.2 Energy Conditions

We verify whether all the energy conditions, like null energy condition (NEC), weak energy condition (WEC), strong energy condition (SEC) and dominant energy condition (DEC), are satisfied at the center ($r = 0$) of the star or not. For this purpose, the following equations should be valid:

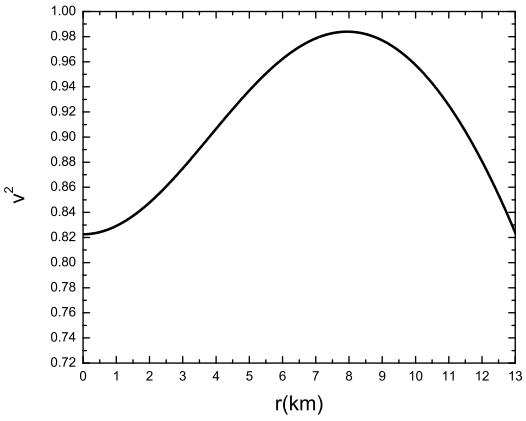

Fig. 4 Speed of sound − radius relationship in the stellar interior (taking $a = 0.0037\,\mathrm{km}^{-2}$, $C = 0.4$).

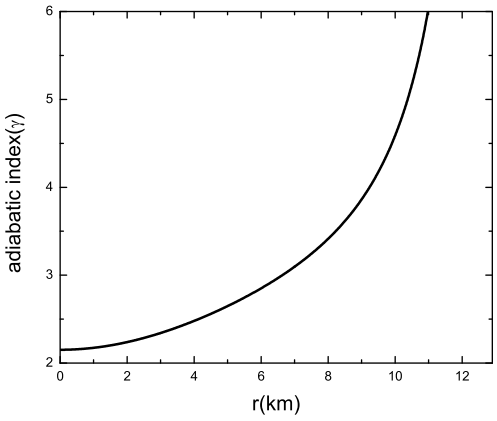

Fig. 5 Relation between adiabatic index γ and the radius of the star in the stellar interior.

(i) NEC: $p_0 + \rho_0 \geq 0$,
(ii) WEC: $p_0 + \rho_0 \geq 0$, $\rho_0 \geq 0$,
(iii) SEC: $p_0 + \rho_0 \geq 0$, $3p_0 + \rho_0 \geq 0$,
(iv) DEC: $\rho_0 > |p_0|$.

From Figures 1 and 2, we observe that all the energy conditions are satisfied (see Table 1).

Table 1 Parameters for Energy Conditions (taking $a = 0.0037\,\mathrm{km}^{-2}$, $C = 0.4$)

ρ_0 (km^{-2})	p_0 (km^{-2})	ρ_0+p_0 (km^{-2})	$3p_0$+ρ_0 (km^{-2})
0.000927945	0.000574442	0.001502387	0.002651271

3.3 Stability

For a physically acceptable model, one expects that the speed of sound should be less than the speed of light ($c = 1$), i.e. within the range $0 \leq v^2 = (\frac{dp}{d\rho}) \leq 1$ (Herrera 1992; Abreu et al. 2007). We plot the speed of sound in Figure 4 and observe that it satisfies the inequality $0 \leq v^2 \leq 1$ everywhere within the stellar object. This verifies the stability of the model.

We also investigate the dynamical stability of the stellar model against the infinitesimal radial adiabatic perturbation which was introduced by Chandrasekhar (1964). Later, this stability condition was gradually developed and applied to astrophysical cases by Bardeen et al. (1966); Knutsen (1988); Mak & Harko (2013). The adiabatic index (γ) is defined as

$$\gamma = \frac{\rho + p}{p}\frac{dp}{d\rho}\,. \tag{8}$$

Since γ should be $> \frac{4}{3}$ everywhere within a stable isotropic star, we plot the adiabatic index for our model (Fig. 5) and observe that $\gamma > \frac{4}{3}$ everywhere within the star. Therefore this stellar model is stable against infinitesimal radial adiabatic perturbations.

3.4 Matching Conditions

The interior metric of the star should be matched to the exterior Schwarzschild metric at the boundary ($r = b$). Continuity of the metric functions across the boundary surface yields

$$e^{\nu} = 1 - \frac{2M}{b} = A^2\left(1 + ab^2\right)^3, \tag{9}$$

$$\begin{aligned} e^{-\lambda} &= \left(1 - \frac{2M}{b}\right) \\ &= \left[1 - \frac{3ab^2}{2}\left(\frac{1 + C(1 + 4ab^2)^{-1/2}}{1 + ab^2}\right)\right]. \end{aligned} \tag{10}$$

Therefore, we can derive the compactification factor from the above equations as

$$\frac{M}{b} = \frac{3}{4}\frac{ab^2(C + \sqrt{1 + 4ab^2})}{(1 + ab^2)\sqrt{1 + 4ab^2}}. \tag{11}$$

3.5 Mass-Radius Relation and Surface Redshift

According to Buchdahl (1959), for a static spherically symmetric perfect fluid sphere, the maximum allowable mass−radius ratio should be $\frac{\mathrm{Mass}}{\mathrm{Radius}} < \frac{4}{9}$. Mak et al. (2001) also proposed a more simplified expression. In

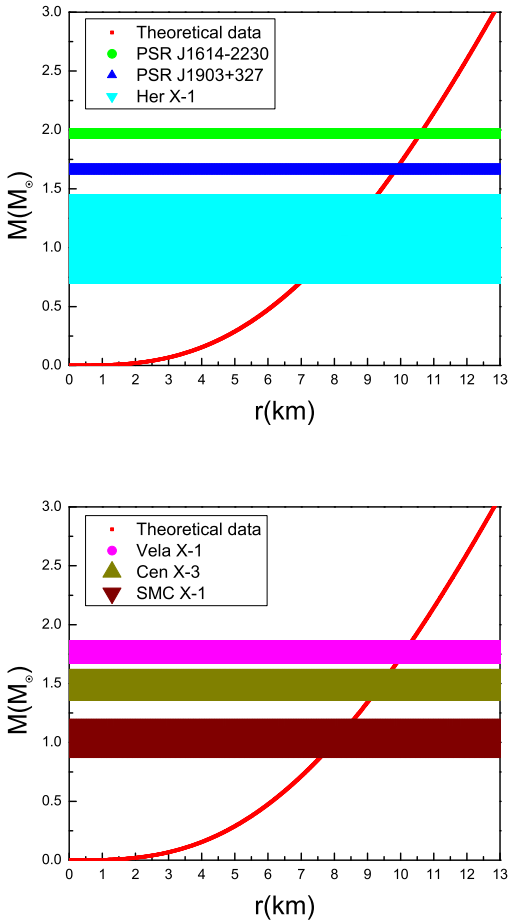

Fig. 6 The predicted mass (M) function of our model with observed data (taking $a = 0.0037\,\mathrm{km}^{-2}$, $C = 0.4$).

our model, the gravitational mass (M) in terms of the matter density (ρ) can be expressed as

$$M = 4\pi \int_0^b \rho\ r^2 dr = \frac{3ab^3\left(C+\sqrt{1+4ab^2}\right)}{4\left(1+ab^2\right)\sqrt{1+4ab^2}}\,, \quad (12)$$

where b is the radius of the star.

The compactness (u) of the star should be

$$u = \frac{M(b)}{b} = \frac{3ab^2\left(C+\sqrt{1+4ab^2}\right)}{4\left(1+ab^2\right)\sqrt{1+4ab^2}}. \quad (13)$$

The mass function and compactness of the star are shown in Figures 6 and 7 respectively.

The surface redshift (Z_s) corresponding to the above compactness (u) can be written as

$$1 + Z_s = \left[1-(2u)\right]^{-\frac{1}{2}}\,, \quad (14)$$

where

$$Z_s = \frac{1}{\sqrt{1-\frac{3ab^2\left(C+\sqrt{1+4ab^2}\right)}{2(1+ab^2)\sqrt{1+4ab^2}}}} - 1\,. \quad (15)$$

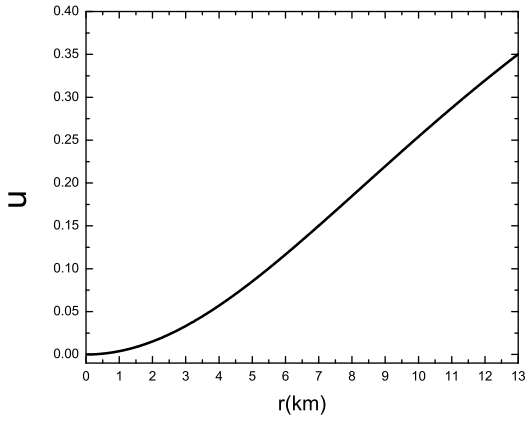

Fig. 7 The compactness (u) in the stellar interior (taking $a = 0.0037\,\mathrm{km}^{-2}$, $C = 0.4$).

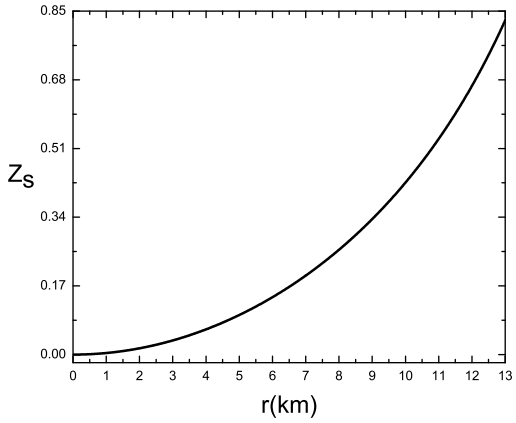

Fig. 8 The redshift function in the stellar interior (taking $a = 0.0037\,\mathrm{km}^{-2}$, $C = 0.4$).

Therefore, from Figure 8, the maximum surface redshift for isotropic neutron stars with different radii can be obtained. Mass, compactness and surface redshift of the neutron stars are evaluated from the above Equations (12), (13) and (15) respectively, and a comparative analysis is done in Table 2.

4 DISCUSSION AND CONCLUDING REMARKS

In this article, we have considered the physical behavior of six compact stars: two binary millisecond pulsars, namely PSR J1614–2230 and PSR J1903+327 studied by Demorest et al. (2010); Freire et al. (2011), and four X-ray binaries, namely Cen X-3, SMC X-1, Vela X-1 and Her X-1, studied by Rawls et al. (2011), by examining

Table 2 Parameter values evaluated in this model (taking $a = 0.0037\,\mathrm{km}^{-2}$, $C = 0.4$). The star's radius and mass (observed) used in this table are taken from the following references: Demorest et al. (2010); Freire et al. (2011); Rawls et al. (2011); Coe et al. (2013); Rahaman et al. (2014).

Star	Radius (km)	Observed Mass ($M_\odot$)	Mass from Model ($M_\odot$)	Redshift	Compactness
PSR J1614–2230	10.3	1.97 ± 0.04	1.84466	0.4560	0.2641
Vela X-1	9.99	1.77 ± 0.08	1.71803	0.4246	0.2536
PSR J1903+327	9.82	1.667 ± 0.021	1.6502	0.4082	0.2478
Cen X-3	9.51	1.49 ± 0.08	1.52955	0.3794	0.2372
SMC X-1	9.13	1.04 ± 0.09	1.38718	0.3462	0.2241
Her X-1	7.7	1.073 ± 0.36	0.910005	0.2390	0.1743

the nature of isotropic pressure and the metric described by Heintzmann (1969).

For a binary system, Jacoby et al. (2005) and Verbiest et al. (2008) used the detection of Shapiro delay to measure the masses of both the neutron star and its companion. Using the same approach, Demorest et al. (2010) performed radio timing observations for the binary millisecond pulsar PSR J1614–2230. The measured mass for the above pulsar is $1.97 \pm 0.04\,M_\odot$. With the help of Arecibo and Green Bank radio timing observations and also considering the relativistic Shapiro delay, Freire et al. (2011) obtained new constraints on the mass of the pulsar and its companion and derived an accurate mass for PSR J1903+327 of $1.667 \pm 0.021\,M_\odot$ through a detailed analysis. Rawls et al. (2011) determined the mass of neutron stars such as Vela X-1, Cen X-3, SMC X-1 and Her X-1 in eclipsing X-ray pulsar binaries. Their measured values are $1.77 \pm 0.08\,M_\odot$ for Vela X-1, $1.49 \pm 0.08\,M_\odot$ for Cen X-3, $1.04 \pm 0.09\,M_\odot$ for SMC X-1 and $1.073 \pm 0.36\,M_\odot$ for Her X-1. Although similar data for other stars are available, we will restrict our discussions to these six stars.

Observed mass, calculated mass, compactness and surface redshift of the above mentioned compact stars are shown in Table 2.

We have obtained quite interesting results from this model, which are summarized as follows:

(i) The solutions are regular at the origin.

(ii) Matter density and pressure variations at the interior of the neutron stars are well behaved (being positive definite at the origin, as illustrated in Figures 1 and 2). Both pressure and matter density are monotonically decreasing to the boundary.

(iii) Pressure is reduced to zero at the boundary (for our model star, it is at 12.9312 km).

(iv) While solving Einstein's equations, we set $c = G = 1$. Now, plugging G and c into the relevant expressions, the values of central density (ρ_0), surface density (ρ_b) and central pressure (p_0) in our model star turn out to be $\rho_0 = 1.2515 \times 10^{15}\,\mathrm{gm\,cm}^{-3}$, $\rho_\mathrm{b} = 0.4717 \times 10^{15}\,\mathrm{gm\,cm}^{-3}$ and $p_0 = 14.3428 \times 10^{35}\,\mathrm{dyne\,cm}^{-2}$ for numerical values of the parameters $b = 12.9312\mathrm{km}$, $a = 0.0037\,\mathrm{km}^{-2}$ and $C = 0.4$.

(v) For our model star, maximum mass of the neutron star comes out as $M_\mathrm{max} = 3.052\,M_\odot < 3.2\,M_\odot$ which is physically acceptable (Rhoades & Ruffini 1974).

(vi) It satisfies stellar equation and energy conditions. Also, it satisfies Herrera's stability criteria (Herrera 1992) and is stable with respect to infinitesimal radial perturbations (Chandrasekhar 1964; Bardeen et al. 1966; Knutsen 1988; Mak & Harko 2013).

(vii) Our model satisfies the Buchdahl mass−radius relation ($\frac{\mathrm{Mass}}{\mathrm{Radius}} < \frac{4}{9}$) (Buchdahl 1959) and from this mass−radius relation (12, 13), some important desired interior features of our model star can be evaluated.

(viii) According to our model, the surface redshift of the neutron stars is found to be within the standard value, i.e. $Z_s \leq 0.85$, which is satisfactory (Haensel et al. 2000).

(ix) From Figure 6 it is clear that our derived mass function is acceptable as the observed masses of various neutron stars are lying on the graph.

(x) We also give two possible EOSs of matter in the interior of the star; one is polynomial (Fig. 9) and the other is exponential (Fig. 10). But using the curve fitting analysis, we see that the best fitted EOS is exponential. We also estimate our model neutron star's EOS and it comes out as $p = \alpha e^{(-\rho/\beta)} + \eta e^{(-\rho/\delta)} +$

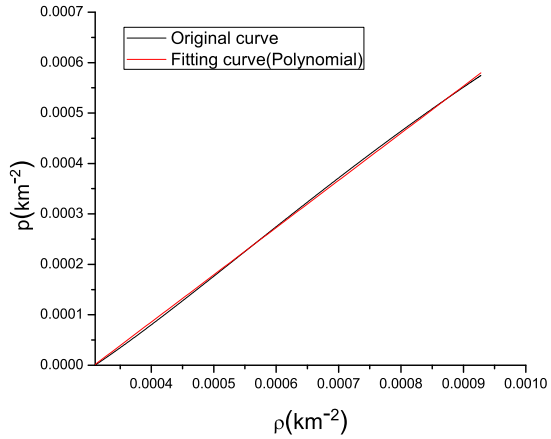

Fig. 9 Polynomial approximation of the pressure (p) – matter density (ρ) relation.

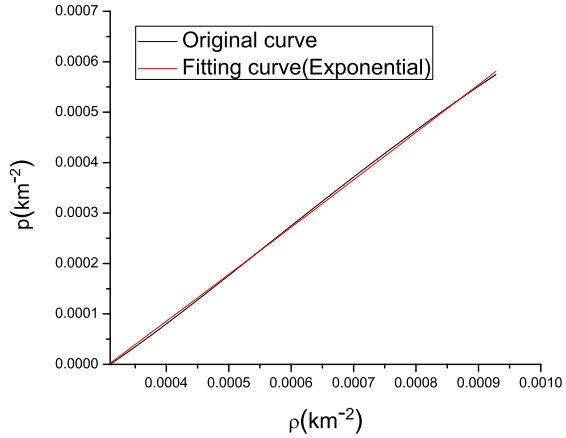

Fig. 10 Exponential approximation of the pressure (p) – matter density (ρ) relation.

ξ, where $\alpha, \beta,\ \eta,\ \delta$ and ξ are constants and interestingly this EOS (Fig. 11) should not be a soft EOS, but rather it would be a stiff EOS, which is also evidently proved in the result of Özel (2006), Guo et al. (2014) and Lai & Xu (2009).

Therefore, we observe that the mass, central density, central pressure, surface density, surface redshift, compactness and EOS of our neutron star model is almost consistent with the investigated millisecond pulsars and X-ray binaries. Therefore our model is applicable to millisecond pulsars and X-ray binaries like PSR J1614–2230, PSR J1903+327, Cen X-3, SMC X-1, Vela X-1 and Her X-1. Hence we can conclude with the hope that it may also be helpful for analyzing other pulsars and X-

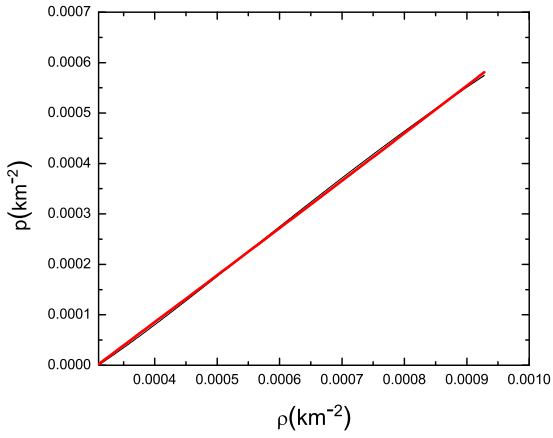

Fig. 11 Pressure (p) – density (ρ) relation (possible EOS) at the stellar interior $p = \alpha e^{(-\rho/\beta)} + \eta e^{(-\rho/\delta)} + \xi$, where $\alpha, \beta, \eta, \delta$ and ξ are constants and all are in units of km^{-2} (taking $a = 0.0037\ \mathrm{km}^{-2}$, $C = 0.4$).

ray binaries. Here we specially want to mention that, very recently, Abbott et al. (2017) found that the dimensionless tidal polarizability, $\Lambda \propto k_2(R/m)^5$ (where k_2 is the second Love number, R is the stellar radius and m is the stellar mass), of stars with $\sim 1.4\ M_\odot$ should be smaller than $\sim\ 1000$. We think that our model presented here could pass this examination since the radius is smaller as mass decreases. (In our model Fig. 6 is similar to fig. 5 in Abbott et al. 2017.)

Acknowledgements MK and SMH gratefully acknowledge the support from IUCAA, in Pune, India and IMSc, in Chennai, India for providing research facilities under the Visiting Associateship Programme, where a part of this work was carried out. We are thankful to the anonymous referee for valuable suggestions that improved the manuscript.

References

Abbott, B. P., Abbott, R., Abbott, T. D., et al. 2017, Physical Review Letters, 119, 161101

Abreu, H., Hernández, H., & Núñez, L. A. 2007, Classical and Quantum Gravity, 24, 4631

Alcock, C., Farhi, E., & Olinto, A. 1986, ApJ, 310, 261

Bardeen, J. M., Thorne, K. S., & Meltzer, D. W. 1966, ApJ, 145, 505

Bhar, P., & Rahaman, F. 2015, European Physical Journal C, 75, 41

Bronnikov, K. A., & Fabris, J. C. 2006, Physical Review Letters, 96, 251101

Buchdahl, H. A. 1959, Physical Review, 116, 1027

Chandrasekhar, S. 1964, ApJ, 140, 417
Coe, M. J., Angus, R., Orosz, J. A., & Udalski, A. 2013, MNRAS, 433, 746
Dayanandan, B., Maurya, S. K., Gupta, Y. K., & Smitha, T. T. 2016, Ap&SS, 361, 160
Demorest, P. B., Pennucci, T., Ransom, S. M., Roberts, M. S. E., & Hessels, J. W. T. 2010, Nature, 467, 1081
Drago, A., Lavagno, A., & Pagliara, G. 2014, Phys. Rev. D, 89, 043014
Dymnikova, I. 2002, Classical and Quantum Gravity, 19, 725
Egeland, E. 2007, Compact Star, Trondheim, Norway
Freire, P. C. C., Bassa, C. G., Wex, N., et al. 2011, MNRAS, 412, 2763
Guo, Y.-J., Lai, X.-Y., & Xu, R.-X. 2014, Chinese Physics C, 38, 055101
Haensel, P., Lasota, J. P., & Zdunik, J. L. 2000, Nuclear Physics B Proceedings Supplements, 80, 11
Haensel, P., Zdunik, J. L., & Schaefer, R. 1986, A&A, 160, 121
Heap, S. R., & Corcoran, M. F. 1992, ApJ, 387, 340
Heintzmann, H. 1969, Zeitschrift fur Physik, 228, 489
Herrera, L. 1992, Physics Letters A, 165, 206
Hossein, S. M., Rahaman, F., Naskar, J., Kalam, M., & Ray, S. 2012, International Journal of Modern Physics D, 21, 1250088
Hossein, S. M., Farhad, N., Molla, S., & Kalam, M. 2016, Ap&SS, 361, 203
Jacoby, B. A., Hotan, A., Bailes, M., Ord, S., & Kulkarni, S. R. 2005, ApJ, 629, L113
Kalam, M., Rahaman, F., Ray, S., et al. 2012, European Physical Journal C, 72, 2248
Kalam, M., Rahaman, F., Monowar Hossein, S., & Ray, S. 2013a, European Physical Journal C, 73, 2409
Kalam, M., Usmani, A. A., Rahaman, F., et al. 2013b, International Journal of Theoretical Physics, 52, 3319
Kalam, M., Monowar Hossein, S., & Molla, S. 2014a, arXiv:1410.0199
Kalam, M., Rahaman, F., Molla, S., & Hossein, S. M. 2014b, Ap&SS, 349, 865
Kalam, M., Rahaman, F., Molla, S., Jafry, M. A. K., & Hossein, S. M. 2014c, European Physical Journal C, 74, 2971
Knutsen, H. 1988, MNRAS, 232, 163
Lai, X., & Xu, R. 2017, in Journal of Physics Conference Series, 861, 012027
Lai, X. Y., & Xu, R. X. 2009, MNRAS, 398, L31
Lattimer, J. M., & Prakash, M. 2005, Physical Review Letters, 94, 111101
Lobo, F. S. N. 2006, Classical and Quantum Gravity, 23, 1525
Maharaj, S., Sunzu, J., & Ray, S. 2014, The European Physical Journal Plus, 129, 3
Mak, M. K., Dobson, Jr., P. N., & Harko, T. 2001, EPL (Europhysics Letters), 55, 310
Mak, M. K., & Harko, T. 2013, European Physical Journal C, 73, 2585
Maurya, S. K., Gupta, Y. K., Dayanandan, B., & Ray, S. 2016, European Physical Journal C, 76, 266
Ngubelanga, S. A., Maharaj, S. D., & Ray, S. 2015, Ap&SS, 357, 74
Orosz, J. A., & Kuulkers, E. 1999, MNRAS, 305, 132
Özel, F. 2006, Nature, 441, 1115
Page, D., Geppert, U., & Weber, F. 2006, Nuclear Physics A, 777, 497
Pant, N., Pradhan, N., & Murad, M. H. 2014, International Journal of Theoretical Physics, 53, 3958
Rahaman, F., Maulick, R., Yadav, A. K., Ray, S., & Sharma, R. 2012a, General Relativity and Gravitation, 44, 107
Rahaman, F., Sharma, R., Ray, S., Maulick, R., & Karar, I. 2012b, European Physical Journal C, 72, 2071
Rahaman, F., Chakraborty, K., Kuhfittig, P. K. F., Shit, G. C., & Rahman, M. 2014, European Physical Journal C, 74, 3126
Rawls, M. L., Orosz, J. A., McClintock, J. E., et al. 2011, ApJ, 730, 25
Rhoades, C. E., & Ruffini, R. 1974, Physical Review Letters, 32, 324
Schaab, C., Hermann, B., Weber, F., & Weigel, M. K. 1997, ApJ, 480, L111
Schwarzschild, K. 1916, Phys.-Math. Klasse, 23, 189
Stickland, D., Lloyd, C., & Radziun-Woodham, A. 1997, MNRAS, 286, L21
Tolman, R. C. 1939, Physical Review, 55, 364
van Kerkwijk, M. H., van Paradijs, J., & Zuiderwijk, E. J. 1995, A&A, 303, 497
Verbiest, J. P. W., Bailes, M., van Straten, W., et al. 2008, ApJ, 679, 675
Weber, F. 2005, Progress in Particle and Nuclear Physics, 54, 193
Witten, E. 1984, Phys. Rev. D, 30, 272